Iranian Journal of Microbiology
Volume 18 Number 2 (April 2026) 268-278
DOI: http://doi.org/10.18502/ijm.v18i2.21304

ORIGINAL ARTICLE

Synthesis and characterization of silica nano particles-based imprinted polymers for detection of herpes simplex virus type 1 in human plasma

Mona Seyed Attaran[1], Seyed Masoud Hosseini[1], Zohreh Sharifi[2*], Mehdi Jahanfar[3*]

[1]Department of Microbiology and Microbial Biotechnology, Faculty of Life Sciences and Biotechnology, Shahid Beheshti University, Tehran, Iran
[2]Biological Products and Blood Safety Research Center, High Institute for Research and Education in Transfusion Medicine, Tehran, Iran
[3]Department of Molecular and Cell Biology, Faculty of Life Sciences and Biotechnology, Shahid Beheshti University, Tehran, Iran

Received: October 2025**, Accepted:** February 2026

ABSTRACT

Background and Objectives: Molecularly imprinted polymers (MIPs) are polymers designed to selectively recognize specific molecules or related compounds. They are created using template molecules, which are later removed, leaving behind cavities tailored to the template's structure. This study aimed to synthesize MIPs for detecting HSV-1 suspended in Human plasma.

Materials and Methods: For synthesizing Silica Nanoparticles and virus-imprinted particles, the Stöber and Sol-gel methods were employed to detect HSV-1 in human plasma. Moreover, ultra-sonication for washing and removal of HSV-1 from VIP, and FESEM were used to determine the shape, size, and characteristics of the synthesized particles. Additionally, DLS was used to confirm the size of particles. MTT assay was employed for cell viability, and TCID50/ml was used for measuring infectious viral titer. Real-time PCR as a molecular assay for virus genome quantification was applied.

Results: The average size of gold-coated freeze-dried SNPs and VIPs was analyzed by FESEM, and the results were 332 and 390 nm, respectively. DLS results showed an average size of 362, 521, and 648 nm for SNPs, VIPs, and NIPs. The VIP cavity size was 156 nm, which was specific for HSV-1. The Real-time PCR confirmed the removal of HSV-1.

Conclusion: The imprinted particles could specifically bind to HSV-1.

Keywords: Herpes simplex virus type 1; Viruses; Molecular imprinting; Silicon dioxide; Nanoparticles; Plasma

INTRODUCTION

Ongoing developments in medicine and biotechnology demand novel immunoassays, biosensors, imaging techniques, and related tools for the diagnosis and treatment of diseases (1). Among the promising approaches, the creation of synthetic nanomaterials capable of molecular recognition has emerged as a prominent research area in chemical sciences, with broad applications spanning medical diagnos-

*Corresponding authors: Zohreh Sharifi, Ph.D, Biological Products and Blood Safety Research Center, High Institute for Research and Education in Transfusion Medicine, Tehran, Iran. Tel: +98-9125172130 Email: z.sharifi@ibto.ir

Mehdi Jahanfar, Ph.D, Department of Molecular and Cell Biology, Faculty of Life Sciences and Biotechnology, Shahid Beheshti University, Tehran, Iran. Tel: +98-9120190857 Email: m_jahanfar@sbu.ac.ir

tics, environmental monitoring, and national security. Since the advent of supramolecular chemistry in the 1980s, extensive work has focused on engineering molecules with precise and predictable recognition functions (2). Molecularly imprinted polymers (MIPs) act as synthetic analogs of antibodies and are synthesized through the co-polymerization of functional monomers and cross-linkers around a target antigen or its derivative, referred to as the template. These templates may include proteins, peptides, lipids, amino acids, viruses, cells, nucleic acids, or more complex glycan structures (3). Functional groups on the polymer chains interact with the template, followed by addition of a cross-linker to covalently link polymer chains at positions not engaged in template binding. Removal of the template generates a polymeric matrix containing cavities that are complementary in size, shape, and chemical functionality to the imprinted target (4). Owing to these unique physicochemical characteristics, MIPs have attracted increasing attention in diverse fields, including separation science, purification processes, biosensing, catalysis, and targeted drug delivery. Numerous studies have demonstrated that MIPs can function as selective recognition elements in immunoassay-based systems, effectively mimicking natural antibodies (5). Viral and bacterial infections pose a substantial burden on global healthcare systems and economies. Seasonal influenza alone accounts for an estimated 250,000–500,000 deaths worldwide each year (6), while cases such as COVID-19 infection, or severe conditions resulting from bacterial and viral contamination of water and food, highlight the importance of early and accurate detection (7-11).

Currently, the most commonly used viral detection methods, such as ELISA and PCR, offer high sensitivity and reliability but are often time-consuming, costly, and require skilled personnel. Consequently, there remains a need for rapid, sensitive, selective, and economical detection methods accessible to end-users (12-14). Among MIP platforms, silica-based viral imprinted polymers (VIPs) inherit the inherent stability of silica nanoparticles, exhibiting robust resistance during storage and operational conditions. These features make them particularly suitable for reliable biomedical and diagnostic applications (15). Molecular imprinting technology integrated with biosensors has recently been suggested as an effective strategy for detecting bacterial and viral pathogens, offering high sensitivity and specificity in a streamlined platform (14).

For example, Uzun et al. (2009) proposed a surface plasmon resonance (SPR) sensor chip incorporating HBsAb-imprinted PHEMAT films for the analysis and purification of HBsAb from human serum. The SPR-based sensor exhibited performance equivalent to the conventional ELISA assay, and no detectable response was observed with HBsAb-negative serum, confirming its selectivity (16, 17). During the SARS-CoV-2 pandemic, MIP-based sensors emerged as promising tools for virus detection due to their ability to specifically bind the receptor-binding domain of the viral spike protein. Carefully selected polymers combined with CoV-specific antibodies function as sensing elements, enabling accurate viral identification (18, 19). Monoclonal-type MIP antibodies further show biocompatibility and potential for COVID-19 treatment, as they can inhibit viral spike protein function and, when combined with antiviral agents, offer targeted drug delivery. Additionally, MIP-based immuno-protective sensors or vaccine candidates may be employed for SARS-CoV-2 detection (19, 20).

Herpesviruses constitute a major family of large, DNA-enveloped viruses. Herpes simplex virus (HSV) was the first human herpesvirus identified and can establish latent infections, leading to asymptomatic recurrences (21). Due to its structural resemblance to the hepatitis B virus (HBV) and its capacity for propagation in vitro, HSV-1 was employed in the present study as a model virus.

This study aimed to synthesize HSV-1-imprinted silica VIPs for the selective detection of HSV-1 in human plasma.

MATERIALS AND METHODS

Virus and cell line. Herpes simplex virus 1 (HSV-1) was used as a live, enveloped DNA virus and was supplied by the Virology Laboratory of the Iran Blood Transfusion Research Center (22). The virus was propagated in African Green Monkey Kidney (Vero) cells obtained from the National Cell Bank of Iran (NCBI, Pasteur Institute; Code: C101). Cells were cultured as monolayers in Dulbecco's Modified Eagle Medium (DMEM, Gibco, UK) supplemented with 5% fetal bovine serum (FBS, Gibco) and 1% penicillin-streptomycin (Sigma), and maintained at 37°C in a humidified atmosphere containing 5% CO_2. All cell

culture and viral manipulations were performed in a certified Class II biosafety cabinet, following Biosafety Level 2 (BSL-2) guidelines to prevent contamination and ensure operator safety. Work surfaces and equipment were disinfected with 70% ethanol prior to use. Biological waste, including spent media and contaminated consumables was collected in biohazard bags and either autoclaved or chemically inactivated, while non-contaminated materials were disposed of separately according to institutional guidelines.

Silica nanoparticles – SNPs – synthesis. Silica synthesis was carried out using TEOS ([TEOS] = 0.22–1.24 M), ammonia ([NH_3] = 0.81 [TEOS]), and water ([H_2O] = 6.25 [TEOS]) in isopropanol. Water (12,520 µL), ammonia (1,680 µL), and isopropanol (12,520 µL) were stirred magnetically at 30 × g for 10 min. TEOS (24,860 µL) was then added dropwise under stirring at 13 × g. The solution gradually turned turbid as silica particles formed and was stirred continuously for 5 h. The resulting particles were centrifuged at 1,699 × g for 10 min, separated, and washed four times with water and ethanol under the same conditions. Then, they were dried in an oven at 150°C for 5 h before the characterization. The size and morphology of the resulting particles were determined with a field emission scanning electron microscope (FESEM, JEOL JSM-7500F, Japan, TESCAN MIRA3 and TESCAN MIRAII, Czech Republic) and Dynamic Light Scattering (Malvern ZETASIZER Nano – ZS).

Virus-imprinted particles – VIPs – synthesis. VIPs were synthesized via the Stöber method, which was chosen for its ability to produce highly monodisperse silica nanoparticles (SNPs) with controlled size and morphology, facilitating the formation of well-defined imprinted cavities and robust template binding. Additionally, the silica matrix provides high chemical and thermal stability, making it suitable for biomedical applications. This approach follows the procedures described by Joshi et al., 2014 (23). SNPs (3.2 mg/mL) were functionalized with 11 µL APTES in 18 mL water for 30 min. Amino-functionalized SNPs were prepared in 20 mL glass vials under magnetic stirring at 13 × g. Following three washes with nano-pure water, the particles were incubated for 30 min in 18 mL of 1% aqueous glutaraldehyde under identical stirring conditions. In the second round, particles were washed three times with nano-pure water and incubated with model viruses at titers of 0.05×10^7, 0.1×10^7, 0.15×10^7, 0.2×10^7, and 0.25×10^7 $TCID_{50}$/mL for 1 h under magnetic stirring at room temperature. To avoid denaturation or unfolding of viral particles, no washing was performed after virus immobilization. TEOS (18 µL) and APTES (36 µL) were subsequently added, and the reaction continued for 2 h at 13 × g. The particles were washed three times with nano-pure water and stored at 4°C. All centrifugation steps were performed at 3,459 × g for 5 min, with pellets resuspended via ultrasonic treatment for 2 min (220 V, 50 Hz). For virus removal, VIPs were treated with 1 M HCl containing 0.01% Triton-X 100, subjected to an initial 10 min ultrasonic treatment, followed by 30 min magnetic stirring at 30 × g, and a second 30 min ultrasonic treatment. Finally, VIPs were washed three times (2,120 × g, 5 min) and freeze-dried. Non-imprinted polymers (NIPs) were prepared identically, excluding the virus incubation step.

Scanning electron microscopy and particle size measurement: Field-emission-scanning-electron-microscope (FESEM) studies. After freeze-drying SNP and VIP, they were coated with a thin layer of gold and then examined by FESEM to determine size and morphology.

Dynamic light scattering (DLS). After freeze-drying, the silica nanoparticles (SNPs) were dispersed in distilled water (DW) and their hydrodynamic size was measured using a dynamic light scattering (DLS) instrument.

Virus removal treatment: From VIP. Two different approaches were employed to evaluate the most effective method for removing viruses from the virus-imprinted polymers (VIPs). The first method was only centrifugation; the other was sonication and centrifugation. To determine the optimal sonication time, 3 samples with three replicates were applied at different times for 5, 10, 20, 25, and 30 minutes; these sample testing times were obtained experimentally. Then, DNA Extraction was done by the sorbent method. The copy number of HSV in the pellet and supernatant of the samples using the real-time PCR was quantified.

From plasma. Plasma samples and binding assays: Human plasma samples were collected from healthy donors and tested using the ELISA method according

to the IBTO protocol to confirm negativity for HIV, HCV, and HBV. Plasma samples were stored at −40°C until use, and all samples were blood type O-positive. To account for plasma complexity, experiments were performed using multiple plasma lots, and HSV-1 at 10^7 $TCID_{50}$/mL was suspended in 150 µL of plasma and subjected to 10-fold serial dilutions in triplicate. For each dilution, 3.2 mg/mL of VIPs was added and stirred for 3 h at 13 × g, followed by virus removal using ultrasonication. Binding performance was evaluated across different plasma lots and dilution levels to ensure reproducibility and robustness of the VIPs in complex biological matrices.

Reproducibility. HSV-1 binding and removal from VIP, with three replicates per sample, were performed. For the binding step, 150 µL of HSV-1 was added to 3.2 mg/mL VIP under magnetic stirring at 13 × g for 3 hours, followed by centrifugation at 2120 × g for 5 minutes. The resulting pellets and supernatants were stored at -20°C. For removal reproducibility, samples were resuspended in triplicate and subjected to ultrasonic treatment for 5, 10, 20, 25, and 30 minutes. DNA was then extracted using the Sorbent method.

MTT assay for VIP. Vero cells were seeded into 96-well plates and allowed to adhere to the well bottoms. Three VIP samples (0.0008, 0.0016, and 0.0032 g) were added to each well in quadruplicate and incubated for 24 h. The medium was then replaced with RPMI 1640. Subsequently, 10 µL of MTT stock solution (5 mg/mL) was added to each well and incubated at 37°C for 4 h. After incubation, DMSO was added to dissolve the formazan crystals, mixed thoroughly, and incubated for an additional 10 min at 37°C. Absorbance was measured at 570 nm using a microplate reader (BIO-IDEA MTT assay kit).

Virus quantification: Live virus quantification. The 50% Tissue Culture Infectious Dose ($TCID_{50}$) method was used to quantify active HSV-1 (18). The virus was propagated in monolayer cell lines, and infectivity titers were calculated using the Spearman–Kärber method with a seven-fold dilution series, performing four replicate cultures per dilution. Virus stocks were stored at -70°C until use.

Viral genome detection. A 500 µL aliquot of warm lysis buffer was added to 150 µL of each sample. The mixture was incubated in a heat block at 65°C for 10 min. The sorbent was added to the microtubes and mixed on a rotator for 15 min. Samples were then centrifuged at 7,168 × g for 15 s, and the supernatant was discarded. Ethanol was added to the pellet, followed by vortexing and centrifugation at 7,168 × g for 15 s; this wash step was repeated twice. Subsequently, samples were centrifuged at 18,928 × g for 15 s, the supernatant was discarded, and microtubes were placed in a heat block at 65°C for 5-10 min with open caps to dry. A warm elution buffer was added to the dried pellet and thoroughly homogenized. Microtubes were incubated at 65°C for 10 min, vortexed, and centrifuged at 7,168 × g for 15 s. The supernatant was transferred to new microtubes, and the samples were ready for PCR analysis. HSV-1 viral load was quantified using real-time PCR on a Rotor-Gene™ 3000 (Corbett Research). The PCR reaction mixture (15 µL total) contained 7.5 µL of AMPLIQON RealQ Plus 2× Master Mix Green (Low ROX), 1 µL forward primer (UL46 F: 5′-GTTTTCGTAGACCCG-CATCC-3′), 1 µL reverse primer (UL46 R: 5′-ATG-GAAGCCACGTATCTGACG-3′), and 5.5 µL DNA sample extracted using the sorbent method. Amplification was performed using 10-fold serial dilutions of standards under the following cycling conditions: initial denaturation at 95°C for 15 s, followed by 40 cycles of 95°C for 30 s, 52°C for 30 s, and 72°C for 30 s. A melting curve analysis was conducted from 72°C to 95°C, increasing 1°C per step, with a 45 s premelt hold at the first step and 5 s at each subsequent step, monitoring fluorescence on the FAM channel.

RESULTS

Virus titration. The live virus titer was calculated to be $10^{7.0}$ $TCID_{50}$/ml.

SNPs synthesis. The SNPs with an average size of 332 nm were obtained. The produced nanoparticles are shown in Fig. 1.

The optimal concentration of HSV-1 for synthesizing VIP. To confirm the results, 3 samples were prepared with different virus concentrations in three different stages of synthesis: the stage of attaching the virus to the nanoparticle, the stage of separating the virus from the nanoparticle, and VIP. From $10^{7.0}$ $TCID_{50}$/ml, five concentrations of HSV-1 were used, respec-

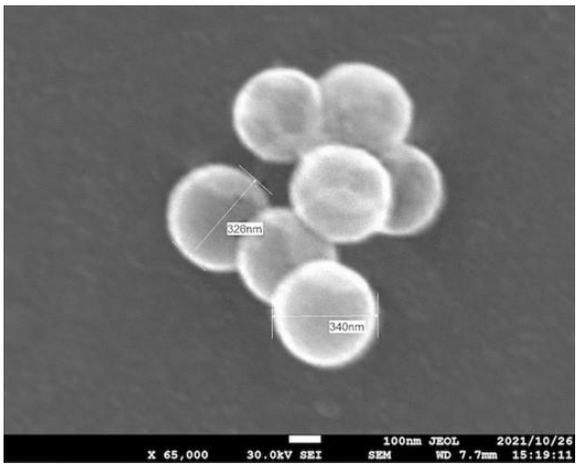

Fig. 1. Characterization of the synthesized silica nanoparticles with the Stöber method using FESEM. Two nanoparticles are shown with diameters of 326 and 340 nm.

tively prepared, as $0.05 \times 10^{7.0}$, $0.1 \times 10^{7.0}$, $0.15 \times 10^{7.0}$, $0.2 \times 10^{7.0}$, and $0.25 \times 10^{7.0}$ $TCID_{50}$/ml for synthesizing VIP. The results demonstrated that VIP synthesis at concentrations of 0.1×10^7 and 0.15×10^7 $TCID_{50}$/mL was effective ($P < 0.0001$). Analysis by electron microscopy and real-time PCR indicated that 0.15×10^7 $TCID_{50}$/mL represents the optimal concentration for VIP synthesis (Figs. 2 and 3).

VIP synthesis. Field-emission scanning electron microscopy (FESEM) analysis revealed that the synthesized VIPs had a mean diameter of 332 nm, while the imprinted cavities corresponding to HSV-1 exhibited a mean diameter of 156 nm, consistent with the dimensions of the virus (Fig. 4).

The synthetic strategy for creating virus recognition sites on the surface of silica nanoparticles (SNPs) is illustrated in Fig. 5.

DLS results. DLS results show an average size of 362, 521, and 648 nm for SNPs, VIPs, and NIPs, respectively, as shown in Fig. 6.

Removal of HSV-1 from VIP. Statistical studies showed a significant difference between the centrifugation and sonication and centrifugation methods (P-value = 0.047); therefore, the use of both methods, sonication and centrifugation, is a good approach for removing the virus from nanoparticles (Fig. 7).

Sonication optimization time for removal of HSV-1 from VIP. To separate the virus from the VIP with the sonication and centrifugation methods, the sonication and centrifugation method according to the obtained results was selected. The results of Real-time PCR showed that in 5-, 10-, and 20-minute sonication, the virus was present in both the supernatant and the pellet, indicating that virus removal was not complete. In 25 minutes of sonication, virus removal was about 107.0 copies/µl, and in 30 minutes of sonication, virus removal was completed (Fig. 8). Statistical analysis with the one-way ANOVA method showed a significant relationship between different times and viral removal (P-value = 0.026).

MTT assay. The optical density (OD) measurements from the control and VIP-treated samples (0.0008, 0.0016, and 0.0032 g) indicated that cell viability decreased with increasing VIP concentration. A one-way ANOVA confirmed a significant difference between the groups (P = 0.0033) (Fig. 9).

DISCUSSION

Human blood remains an indispensable source of therapeutic products that are widely utilized for the prevention and treatment of critical and life-threatening diseases. The findings of this study further highlight the importance of ensuring the safety and efficiency of blood-derived materials, particularly when designing advanced detection or purification systems (24). Nevertheless, blood and plasma derivatives, such as immunoglobulin, carry a risk of contamination by various blood-borne pathogens.

The present study demonstrates that HSV-1–imprinted biosilica nanoparticles synthesized via the Stöber method are comparable to previously reported virion-imprinted systems, while offering improved virus specificity and clinical relevance. Similar to Cumbo et al. (2013), nanoparticles with a comparable overall size (~390–410 nm) were obtained; however, the template virus differed substantially. Cumbo et al. used a small, non-enveloped RNA virus (28–33 nm), resulting in ~20 nm surface cavities, whereas the use of an enveloped DNA virus (HSV-1, 125–130 nm) in this study led to larger imprinted cavities (~156 nm), closely matching the virus dimensions and confirming successful imprinting. Importantly, unlike earlier studies that focused mainly on model systems, the present work demonstrates sensitive virus detection directly from fresh frozen plasma, achieving detec-

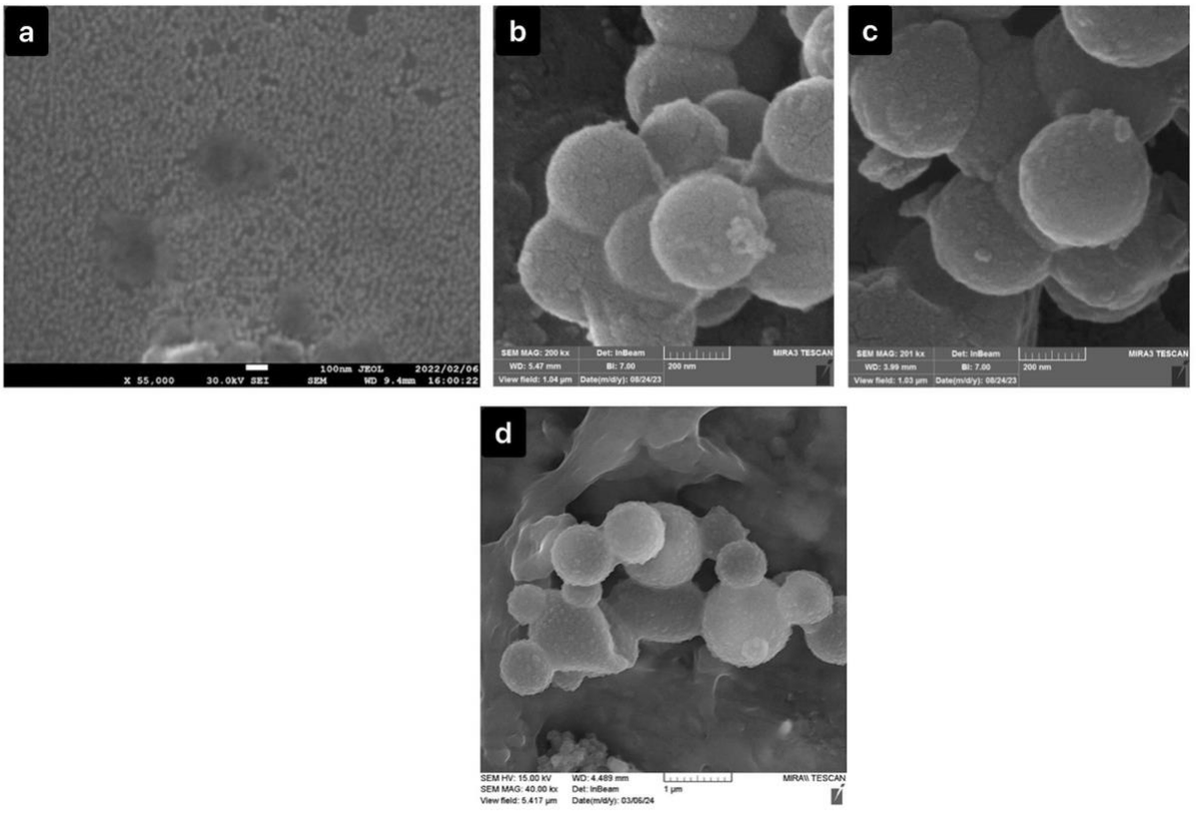

Fig. 2. FESEM images of concentrations (a) $0.15 \times 10^{7.0}$, (b) $0.2 \times 10^{7.0}$, and (c) $0.25 \times 10^{7.0}$ $TCID_{50}$/ml HSV-1 for synthesized VIP and (d) the morphology of NIPs. Due to the low concentration of the virus, the number of cavities created by the virus was low, and therefore, concentrations of $0.05 \times 10^{7.0}$ and $0.1 \times 10^{7.0}$ $TCID_{50}$/ml HSV-1 were not detectable. In the higher concentrations of $0.2 \times 10^{7.0}$, $0.25 \times 10^{7.0}$ $TCID_{50}$/ml HSV-1, due to the lack of homogeneity, two phases of the virus and the VIP were probably formed, and these two did not mix to make the imprints.

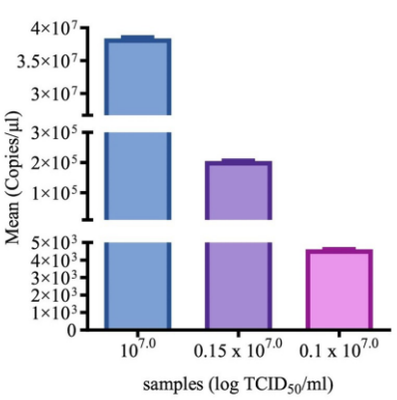

Fig. 3. Real-time PCR results show the optimal concentration of HSV-1 for synthesizing VIP.

tion down to 102.0 copies/µL without observable cytotoxicity. These findings highlight the suitability of biosilica VIPs for selective detection of enveloped viruses in complex biological matrices and their potential application in blood safety monitoring (2).

Waterborne viruses, such as HAV, HEV, Norovirus, and Rotavirus, pose significant public health risks, highlighting the need for effective viral detection and removal. Altintas et al. (2015) demonstrated that MIP-based nanoparticles (205–238 nm) efficiently bound bacteriophage MS2; however, these particles were smaller than the VIPs synthesized in the present study. Here, VIPs were tailored for a larger, enveloped virus (HSV-1) with particle sizes of ~390 nm and cavity dimensions of ~156 nm, enabling sensitive detection directly from plasma (102 copies/µL) without cytotoxic effects. This comparison indicates that molecular imprinting strategies can be successfully extended to larger, clinically relevant viruses, broadening the applicability of VIPs from environmental monitoring to biomedical diagnostics (12).

Adenoviruses cause infections in multiple systems and can be highly transmissible, making rapid detection essential. Gast et al. (2018) showed that surface-passivated imprinted silica nanoparti-

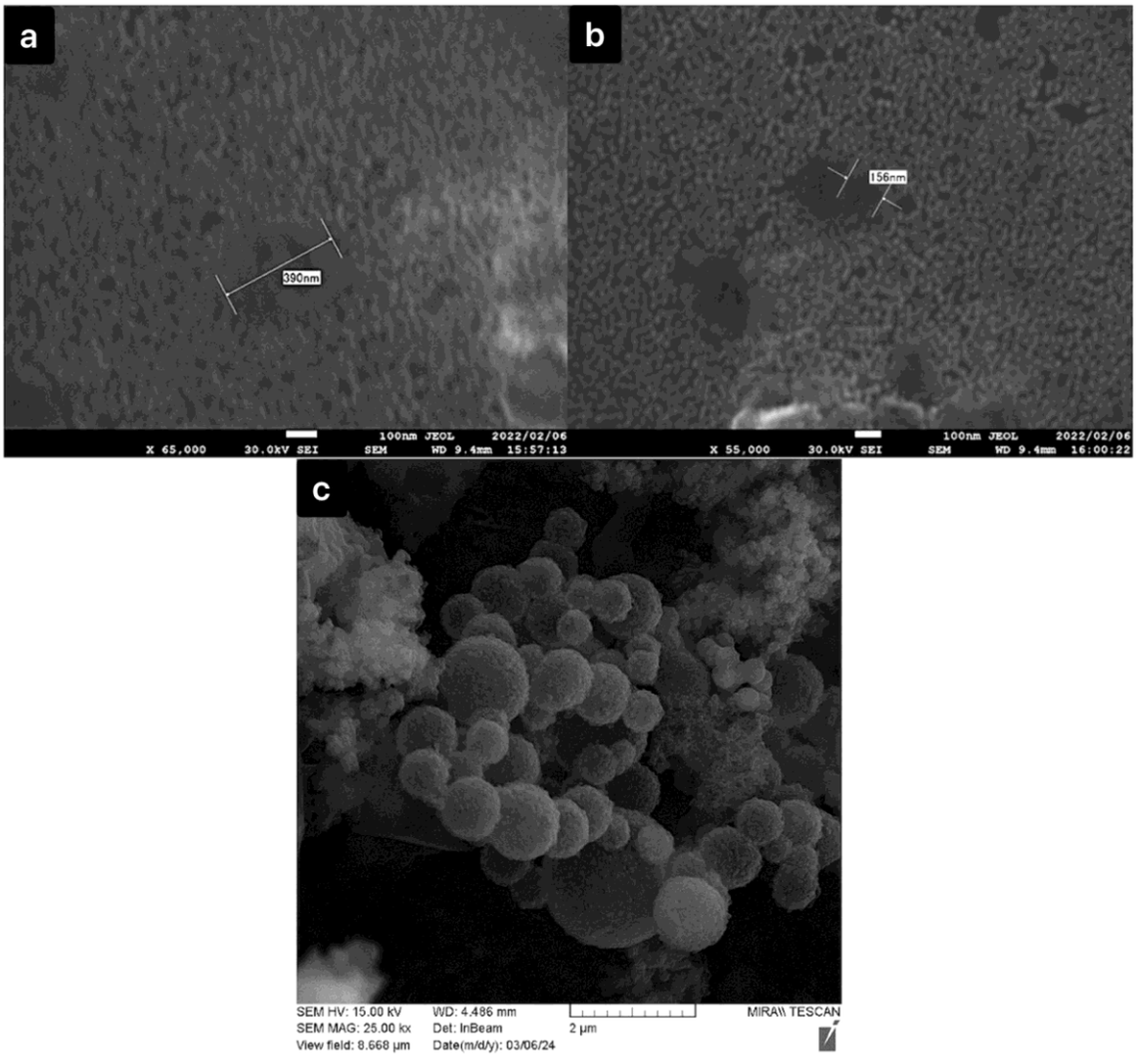

Fig. 4. (a) Synthesized VIP with 390 nm diameter. (b) The imprint of HSV-1. (c) NIPs.

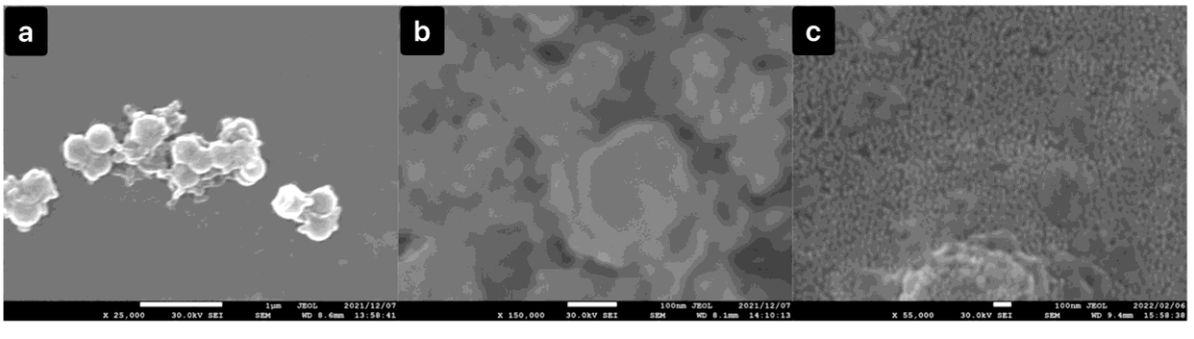

Fig. 5. (a) Immobilization of the target virus on the surface of silica nanoparticles (SNPs). (b) Surface-initiated growth of a polysilsesquioxane layer, referred to as the recognition layer, on silica nanoparticles, and (c) Removal of the template virus, thus freeing the imprints. The final particles are named virus-imprinted particles, or VIPs.

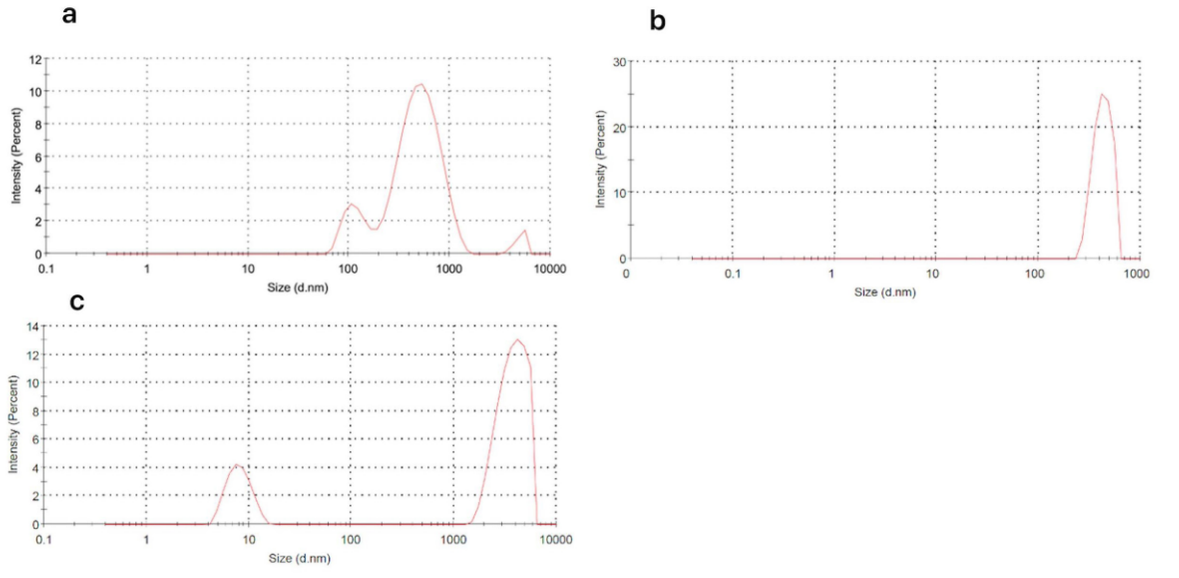

Fig. 6. DLS results for synthesized particles. (a) The z-average was 362 nm, and Pdl was 0.410 for SNP. (b) The z-average was 521 nm, and Pdl was 1.000 for VIP. (c) The z-average was 648 nm, and Pdl was 1.000 for NIP.

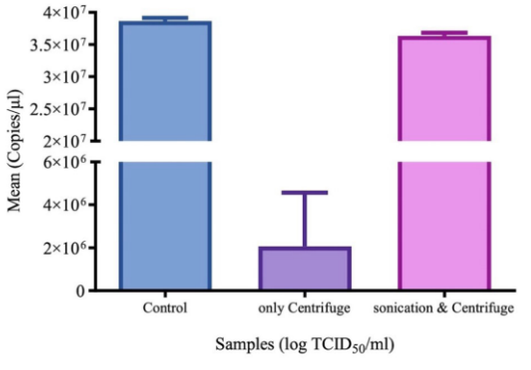

Fig. 7. Supernatant Real-time PCR results for the best method for removing virus from VIP.

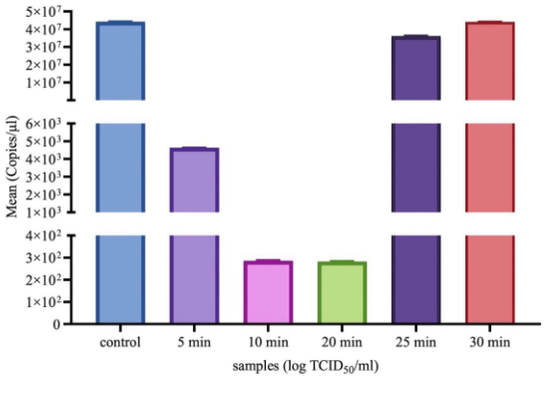

Fig. 8. Supernatant Real-time PCR results for the optimal time by Ultrasonication for virus removal

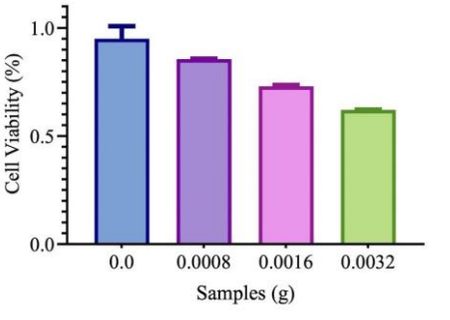

Fig. 9. Optical density for different concentrations of VIP for cell viability

cles (~900 nm) effectively recognized adenovirus (~90 nm), with imprinted cavities accommodating particles of 70–100 nm. In comparison, the VIPs synthesized in our study were smaller in the overall size (~390 nm) but were tailored with cavities (~156 nm) precisely matching the dimensions of our target virus, HSV-1. Despite the size differences, our results demonstrate similarly high virus-specific recognition directly from plasma (102 copies/µL) without cytotoxic effects, highlighting that molecular imprinting can be successfully adapted to different viruses and particle scales while maintaining selectivity and functional performance (25).

Altintas et al. (2015) investigated adenovirus-targeted MIPs (ADV-MIPs) using a prism-based SPR

biosensor, comparing their performance to MIPs against bacteriophage MS2, vancomycin-targeted MIPs, and an adenovirus serotype 5 antibody. ADV-MIPs showed high specificity, confirmed by limited binding to MS2, and had an average particle size of 265 nm, as verified by DLS and TEM. While their synthesis protocols and materials differed from the present study, the ADV-MIPs were smaller than the VIPs produced here (~390 nm with ~156 nm cavities for HSV-1). Despite this size difference, our results demonstrate that tailored VIPs achieve virus-specific recognition and sensitive detection directly from plasma (102 copies/μL), highlighting the adaptability of molecular imprinting for larger, clinically relevant viruses (26).

Yang et al. (2017) developed a resonance light scattering (RLS) sensor by coating SiO_2 nanoparticles (~70 nm) with polydopamine and HAV-imprinted polymers using the Stöber method for specific HAV detection. TEM confirmed the formation of imprinted sites, and the sensor showed high selectivity over other viruses, including rabies vaccine, JEV, and measles-rubella vaccines, with negligible cytotoxicity toward Chinese hamster fibroblast cells. While their silica nanoparticles were larger than those synthesized in the present study, our results similarly confirmed the absence of cytotoxicity for HSV-1 VIPs, supporting the biocompatibility of the tailored imprinted nanoparticles. These findings collectively demonstrate that molecular imprinting can produce highly selective and safe VIPs for viral detection across different virus types and particle sizes (27).

Current methods for dengue virus detection are often complex and time-consuming, limiting their applicability for early epidemiological monitoring. Su et al. (2003) were the first to apply MIP-based strategies for dengue virus using a Quartz Crystal Microbalance (QCM), focusing on optimizing antibody immobilization with protein A, glutaraldehyde, and carbodiimide methods. While their study improved sensitivity and reduced technical complexity, it relied on antibody-based recognition rather than direct viral imprinting. In contrast, the present study develops virus-imprinted polymers (VIPs) for direct recognition of viral particles, eliminating the need for antibodies and offering a simplified, rapid, and selective detection approach. These results highlight the potential of VIPs to complement or replace conventional antibody-based methods for virus detection (28).

Japanese encephalitis virus (JEV) causes viral encephalitis affecting thousands annually, highlighting the need for rapid and cost-effective detection methods. Luo et al. (2019) developed surface-imprinted fluorescent sensors using JEV with Fe_3O_4@SiO_2 magnetic microspheres (~200 nm), demonstrating high specificity against JEV and minimal nonspecific binding, with no cytotoxic effects in cell culture. Although their particle size and synthesis methods differed from the VIPs in the present study, which were larger (~390 nm) and tailored for HSV-1, our results similarly showed selective viral recognition and absence of cytotoxicity. This comparison underscores the versatility of molecular imprinting for producing selective and biocompatible virus-imprinted polymers across different virus types and particle sizes (29).

Wangchareansak et al. (2013) applied molecular imprinting to screen multiple influenza A subtypes (H5N1, H5N3, H1N1, H1N3, and H6N1) using QCM sensors. Influenza A virus particles (80–120 nm) were successfully imprinted, and rebinding was confirmed via AFM, with MIPs fully responding to the template virus. However, the sensors could not distinguish between subtypes, highlighting a limitation in subtype specificity. In contrast, the VIPs developed in the present study for HSV-1 (~125–130 nm, cavity size ~156 nm) demonstrated selective recognition in plasma with no cytotoxicity. This comparison underscores that carefully tailored VIPs can achieve both virus-specific recognition and functional performance in complex biological matrices, extending the applicability of molecular imprinting beyond environmental or subtype-limited assays (30).

Tancharoen et al. (2019) proposed a simple approach for Zika virus (ZIKV) detection using surface-imprinted polymers (SIPs) combined with electrochemical methods and qRT-PCR, achieving a correlation of 5,028 RNA copies per PFU. SEM analysis revealed SIP pores of ~80 nm, smaller than the VIP cores synthesized in the present study. Unlike their method, the present work directly quantified infectious HSV-1 particles using plaque assays and demonstrated selective recognition in plasma with VIPs (~390 nm, cavity size ~156 nm). This comparison highlights that tailored VIPs can provide virus-specific detection in complex biological matrices while maintaining functional performance, complementing existing SIP-based electrochemical approaches (31).

In studies on animal viruses, classical swine fe-

ver virus (CSFV) is often used as a model at concentrations of 10^3 $TCID_{50}$/mL. Klangprapan et al. (2020) investigated MIPs targeting CSFV, characterizing imprinted copolymers with QCM and SEM, revealing surface-bound virus particles (30-60 nm) and post-template removal cavities averaging 59 nm, with strong selectivity over PRRSV and PRV. While the particle sizes in our study were larger, the VIPs developed for HSV-1 (~390 nm, cavity ~156 nm) similarly demonstrated selective viral recognition in plasma and absence of cytotoxicity. This comparison highlights that molecular imprinting can be adapted for viruses of different sizes and origins, providing selective and biocompatible platforms for both research and diagnostic applications (32).

In another study, norovirus virus-like particles (NorVLP) from genotype GII.4 were used for molecular imprinting, with template removal and imprinting procedures similar to those in the present study. Immobilization and growth of the recognition layer were performed in aqueous conditions, and FE-SEM analysis confirmed successful imprinting with spherical structures on the nanoparticle surfaces. The stability of both the recognition layer and imprinted particles was maintained under ultrasonic treatment, demonstrating robust VIPs. Similarly, the HSV-1 VIPs developed in the present study (~390 nm, cavity ~156 nm) showed selective viral recognition and stability in plasma, highlighting that molecular imprinting strategies can reliably produce durable and functional VIPs across different virus types and experimental conditions (33).

CONCLUSION

In this study, monodisperse silica nanoparticles (SNPs) were successfully synthesized via the Stöber method and characterized by FESEM and DLS for size and morphology. Virus-imprinted polymers (VIPs) and non-imprinted polymers (NIPs) were subsequently prepared using sol-gel techniques. The optimal virus concentration for VIP formation was determined through real-time PCR, FESEM, and DLS analyses, while the most effective ultrasonication duration for template removal was also established. The resulting VIPs demonstrated selective binding to HSV-1 in human plasma, highlighting their potential for sensitive virus detection and future applications in biomedical diagnostics and antiviral strategies.

ACKNOWLEDGEMENTS

The authors sincerely thank Mrs. Paz at the IBTO Research Center Virology Laboratory for her technical support. We also extend our gratitude to the Central Laboratory at Shahid Beheshti University (SBU) for providing access to FESEM instrumentation.

REFERENCES

1. Haupt K, Medina Rangel PX, Bui BTS. Molecularly Imprinted Polymers: Antibody Mimics for Bioimaging and Therapy. *Chem Rev* 2020;120:9554-9582.
2. Cumbo A, Lorber B, Corvini PFX, Meier W, Shahgaldian P. A synthetic nanomaterial for virus recognition produced by surface imprinting. *Nat Commun* 2013;4:1503-1507.
3. El-Schich Z, Zhang Y, Feith M, Beyer S, Sternbæk L, Ohlsson L, et al. Molecularly imprinted polymers in biological applications. *Biotechniques* 2020;69:406-419.
4. Bolisay LD, Kofinas P. Imprinted Polymer Hydrogels for the Separation of Viruses. *Macromol Symp* 2010;291–292:302-306.
5. Vasapollo G, Sole R Del, Mergola L, Lazzoi MR, Scardino A, Scorrano S, et al. Molecularly Imprinted Polymers: Present and Future Prospective. *Int J Mol Sci* 2011;12:5908-5945.
6. Choi Y, Hwang JH, Lee SY. Recent Trends in Nanomaterials-Based Colorimetric Detection of Pathogenic Bacteria and Viruses. *Small Methods* 2018; 2(4):1700351.
7. Singh R, Verma R, Kaushik A, Sumana G, Sood S, Gupta RK, et al. Chitosan–iron oxide nano-composite platform for mismatch-discriminating DNA hybridization for Neisseria gonorrhoeae detection causing sexually transmitted disease. *Biosens Bioelectron* 2011;26:2967-2974.
8. Bridle H, Balharry D, Gaiser B, Johnston H. Exploitation of Nanotechnology for the Monitoring of Waterborne Pathogens: State-of-the-Art and Future Research Priorities. Environ. *Sci Technol* 2015;49:10762-1077.
9. Lifson MA, Ozen MO, Inci F, Wang S, Inan H, Baday M, et al. Advances in biosensing strategies for HIV-1 detection, diagnosis, and therapeutic monitoring. *Adv Drug Deliv Rev* 2016;103:90-104.
10. Vidic J, Manzano M, Chang CM, Jaffrezic-Renault N. Advanced biosensors for detection of pathogens related to livestock and poultry. *Vet Res* 2017;48:11.
11. Yoo SM, Lee SY. Optical iosensors for the Detection of Pathogenic Microorganisms. *Trends Biotechnol* 2016;34:7-25.
12. Altintas Z, Gittens M, Guerreiro A, Thompson KA,

Walker J, Piletsky S, et al. Detection of Waterborne Viruses Using High Affinity Molecularly Imprinted Polymers. *Anal Chem* 2015;87:6801-6807.
13. Jia M, Zhang Z, Li J, Ma X, Chen L, Yang X. Molecular imprinting technology for microorganism analysis. *Trac Trends Anal Chem* 2018;106:190-201.
14. Zhang J, Wang Y, Lu X. Molecular imprinting technology for sensing foodborne pathogenic bacteria. *Anal Bioanal Chem* 2021;413:4581-4598.
15. Bruckmann F da S, Nunes FB, Salles T da R, Franco C, Cadoná FC, Bohn Rhoden CR. Biological Applications of Silica-Based Nanoparticles. *Magnetochemistry* 2022;8:131.
16. Uzun L, Say R, Ünal S, Denizli A. Hepatitis B surface antibody purification with hepatitis B surface antibody imprinted poly(hydroxyethyl methacrylate-N-methacryloyl-l-tyrosine methyl ester) particles. *J Chromatogr B Analyt Technol Biomed Life Sci* 2009;877:181-188.
17. Uzun L, Say R, Ünal S, Denizli A. Production of surface plasmon resonance based assay kit for hepatitis diagnosis. *Biosens Bioelectron* 2009;24:2878-2884.
18. Nandy Chatterjee T, Bandyopadhyay R. A Molecularly Imprinted Polymer-Based Technology for Rapid Testing of COVID-19. *Trans Indian Natl Acad Eng* 2020;5:225-228.
19. Refaat D, Aggour MG, Farghali AA, Mahajan R, Wiklander JG, Nicholls IA, et al. Strategies for Molecular Imprinting and the Evolution of MIP Nanoparticles as Plastic Antibodies—Synthesis and Applications. *Int J Mol Sci* 2019; 20: 6304.
20. Parisi OI, Dattilo M, Patitucci F, Malivindi R, Delbue S, Ferrante P, et al. Design and development of plastic antibodies against SARS-CoV-2 RBD based on molecularly imprinted polymers that inhibit in vitro virus infection. *Nanoscale* 2021;13:16885-16899.
21. Patrick R. Murray, Ken S. Rosenthal, Michael A. Pfaller. Medical Microbiology, . 8th ed. In. Elsevier; 2015. p. 426-46.
22. Razani E, Aghayan HR, Alavi-Moghadam S, Yari F, Gharehbaghian A, Sharifi Z. A comparative study of pathogen inactivation technologies in human platelet lysate and its optimal efficiency in human placenta-derived stem cells culture. *J Virol Methods* 2022;302:114478.
23. Joshi S, Rao A, Lehmler HJ, Knutson BL, Rankin SE. Interfacial molecular imprinting of Stöber particle surfaces: A simple approach to targeted saccharide adsorption. *J Colloid Interface Sci* 2014;428:101-110.
24. Kawano M., Breiman R.F., Clemens J., Goldenthal K., Dale Horne A., Kamiya H., et al. World Health Organization, 2004. WHO Technical Report, Series No.924. [Internet]. [cited 2024 Apr 21]. Report. Available from: https://www.who.int/publications/m/item/guidelines-on-clinical-evaluation-of-vaccines-regulatory-expectations
25. Gast M, Kühner S, Sobek H, Walther P, Mizaikoff B. Enhanced Selectivity by Passivation: Molecular Imprints for Viruses with Exceptional Binding Properties. *Anal Chem* 2018;90:5576-5585.
26. Altintas Z, Pocock J, Thompson KA, Tothill IE. Comparative investigations for adenovirus recognition and quantification: Plastic or natural antibodies? *Biosens Bioelectron* 2015;74:996-1004.
27. Yang B, Gong H, Chen C, Chen X, Cai C. A virus resonance light scattering sensor based on mussel-inspired molecularly imprinted polymers for high sensitive and high selective detection of Hepatitis A Virus. *Biosens Bioelectron* 2017;87:679-685.
28. Su CC, Wu TZ, Chen LK, Yang HH, Tai DF. Development of immunochips for the detection of dengue viral antigens. *Anal Chim Acta* 2003;479:117-123.
29. Luo L, Yang J, Liang K, Chen C, Chen X, Cai C. Fast and sensitive detection of Japanese encephalitis virus based on a magnetic molecular imprinted polymer–resonance light scattering sensor. *Talanta* 2019;202:21-26.
30. Wangchareansak T, Thitithanyanont A, Chuakheaw D, Gleeson MP, Lieberzeit PA, Sangma C. Influenza A virus molecularly imprinted polymers and their application in virus sub-type classification. *J Mater Chem B* 2013;1:2190.
31. Tancharoen C, Sukjee W, Thepparit C, Jaimipuk T, Auewarakul P, Thitithanyanont A, et al. Electrochemical Biosensor Based on Surface Imprinting for Zika Virus Detection in Serum. *ACS Sens* 2019;4:69-75.
32. Klangprapan S, Choke-arpornchai B, Lieberzeit PA, Choowongkomon K. Sensing the classical swine fever virus with molecularly imprinted polymer on quartz crystal microbalance. *Heliyon* 2020;6(6):e04137.
33. Sykora S, Cumbo A, Belliot G, Pothier P, Arnal C, Dudal Y, et al. Virus-like particles as virus substitutes to design artificial virus-recognition nanomaterials. *Chem Commun (Camb)* 2015;51:2256-2258.